
Figures and figure supplements

Controlling protein function by fine-tuning conformational flexibility

Sonja Schmid and Thorsten Hugel

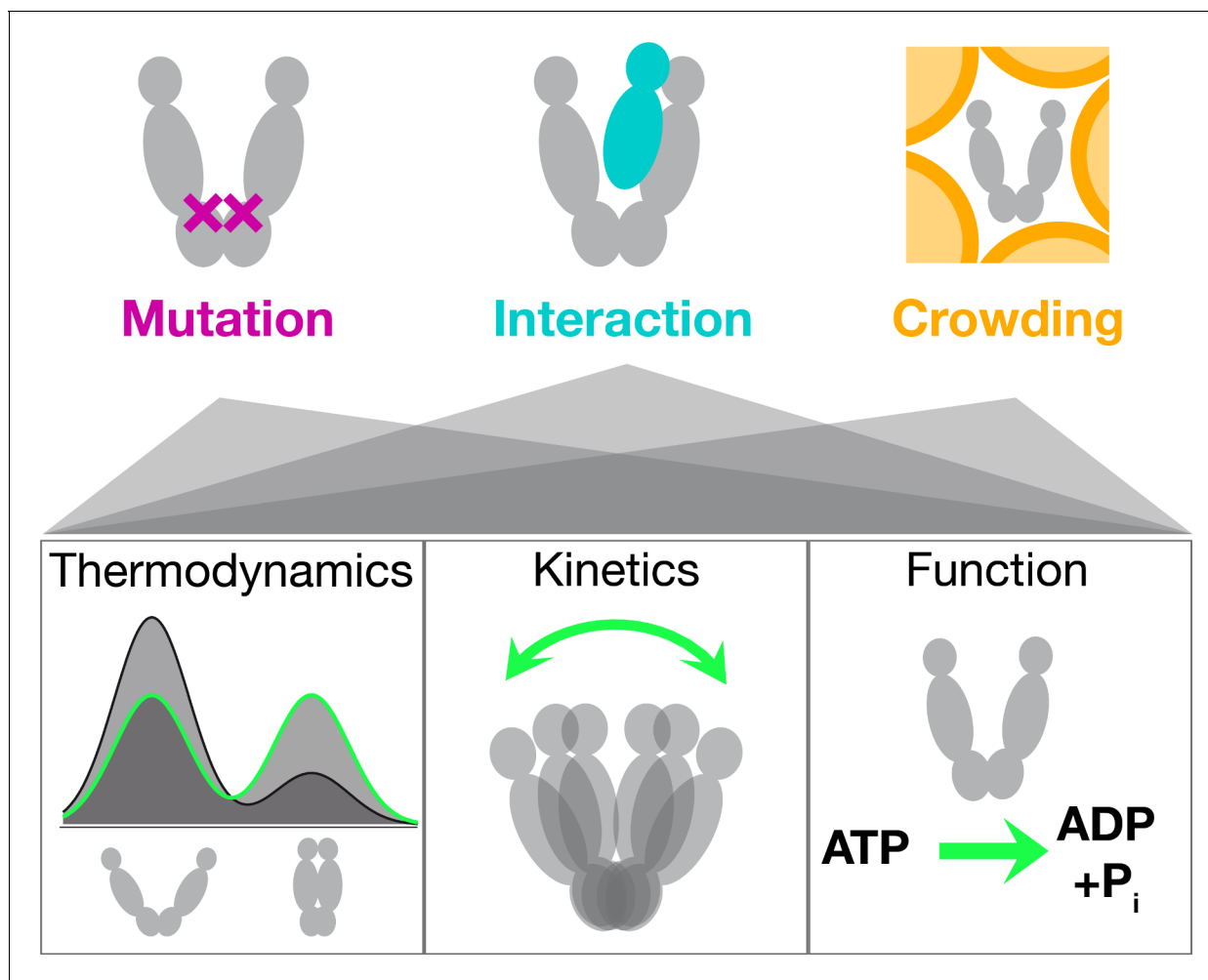


Figure 1. Protein regulation uses different degrees of localization. Mutations or PTMs act most locally, protein-protein interactions (PPIs) act on the protein domain level, and changes in the global environment, such as crowding or phase separation, act non-specifically and globally on the protein. Each of them affects conformational thermodynamics and kinetics to fine-tune the protein conformational state space and thereby protein function.

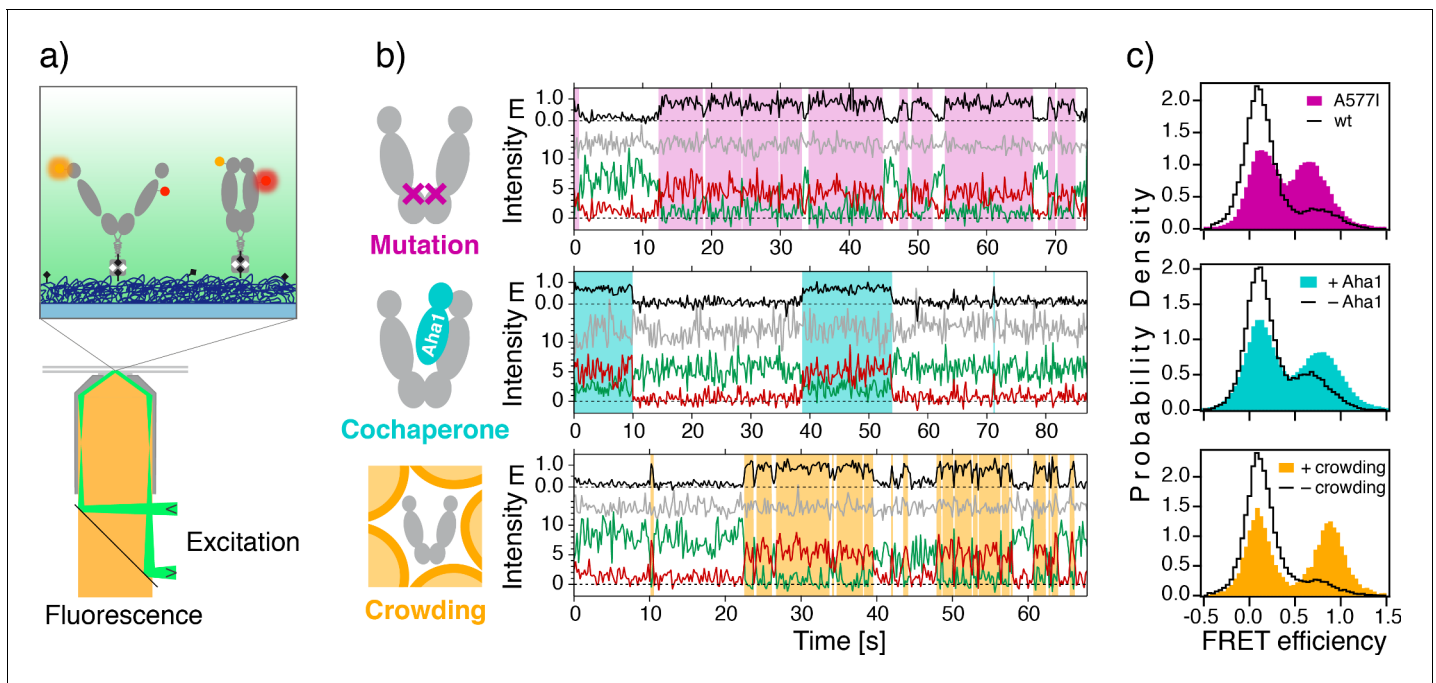


Figure 2. Mutation, cochaperone interaction, and crowding show similar thermodynamic effects. (a) Illustration of the single-molecule FRET experiment using an objective-type TIRF microscope (bottom): cross section through the objective, and flow chamber (both gray) and the dichroic mirror (black) separating the laser excitation (green) from the collected fluorescence (yellow). The zoom view (top) shows the fluorescently labeled Hsp90 (FRET donor, orange; acceptor red), which is immobilized on a PEG-passivated (dark blue) coverslip (light blue) using biotin-neutravidin coupling (black and gray). (b) Example time traces obtained from individual Hsp90 molecules for the point mutant A577I (top), in the presence of 3.5 μ M cochaperone Aha1 (center), or under macro-molecular crowding by 20wt% Ficoll400 (bottom). Depicted are the FRET efficiency E (black), the fluorescence of the FRET donor (green) and acceptor (red) and the directly excited acceptor (gray). White and colored overlays denote low- and high-FRET dwells, respectively, as obtained using a hidden Markov model and the Viterbi algorithm. (c) FRET histograms compiled from many single-molecule trajectories as indicated, and normalized to unity (wt: wild type). Reference data (black) were measured under the specific conditions of each of the three experiment series (see also Materials and methods). Example traces of the reference data are provided in **Figure 2—figure supplement 1**. All fits and fit coefficients for 2 c are shown in **Figure 2—figure supplement 2**. Experimental conditions for A577I or wt Hsp90: 2 mM ATP in 40 mM Hepes, 150 mM KCl, 10 mM MgCl_2 , pH7.5. Conditions with and without 3.5 μ M Aha1: wt Hsp90, 2 mM ATP in 40 mM Hepes, 20 mM KCl, 5 mM MgCl_2 , pH 7.5. Conditions with and without crowding by 20wt% Ficoll400: wt Hsp90 in 40 mM Hepes, 150 mM KCl, 10 mM MgCl_2 , pH7.5. The data were recorded in 5 to 13 videos per dataset, on one or more days. The number of individual molecules included per histogram are: A577I, 154; wt, 163; +Aha1, 366; -Aha1, 231; +crowding, 50; -crowding, 81. All smFRET traces are available from **Figure 2—source data 1**.

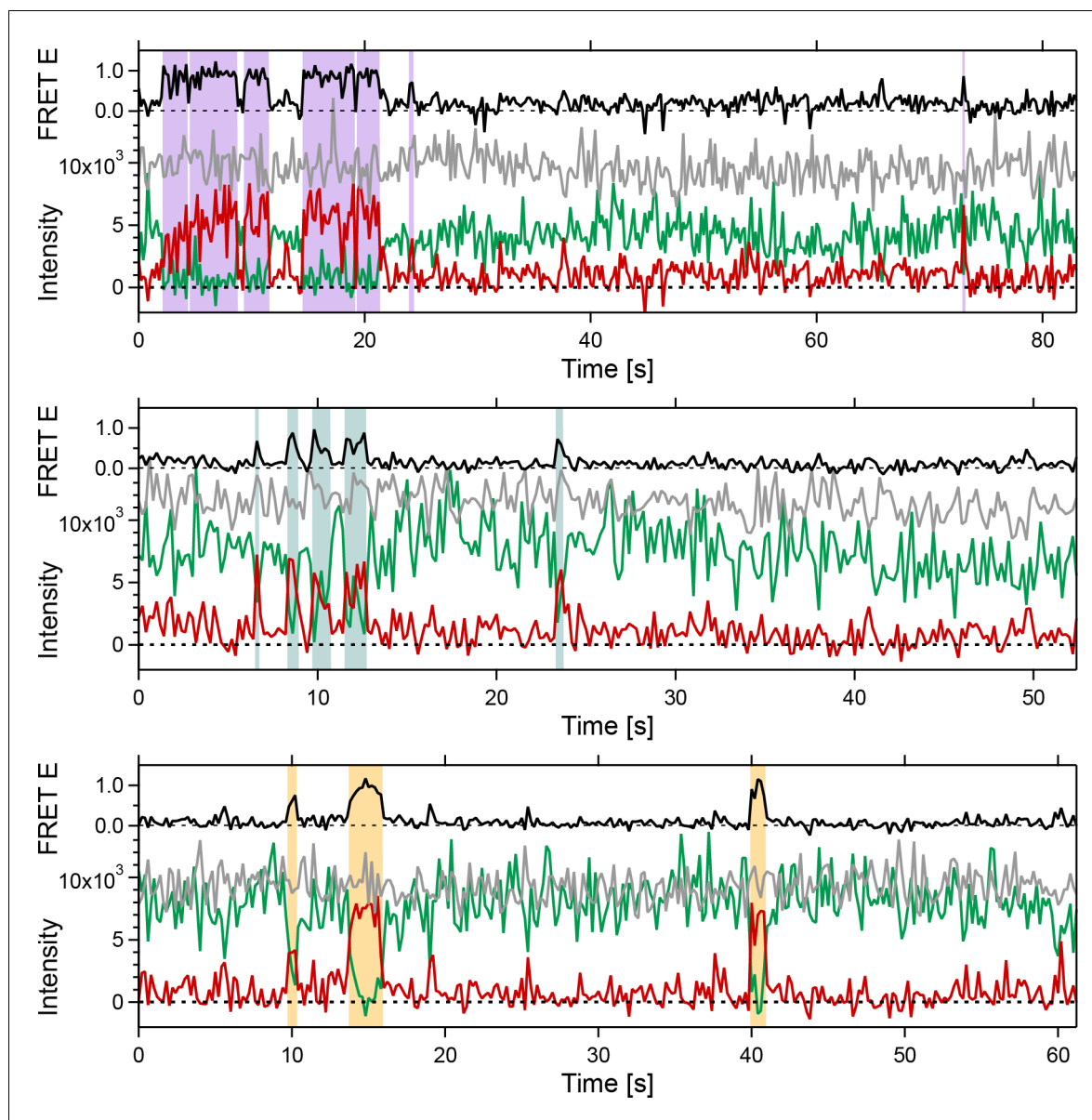


Figure 2—figure supplement 1. Example traces of the reference datasets. Example traces of the three reference datasets (black lines in **Figure 2c**, labeled: wt, -Aha1, -crowding) used for the point mutation, the Aha1 interaction, and macro-molecular crowding (top to bottom). Color code and experimental conditions as in **Figure 2**.

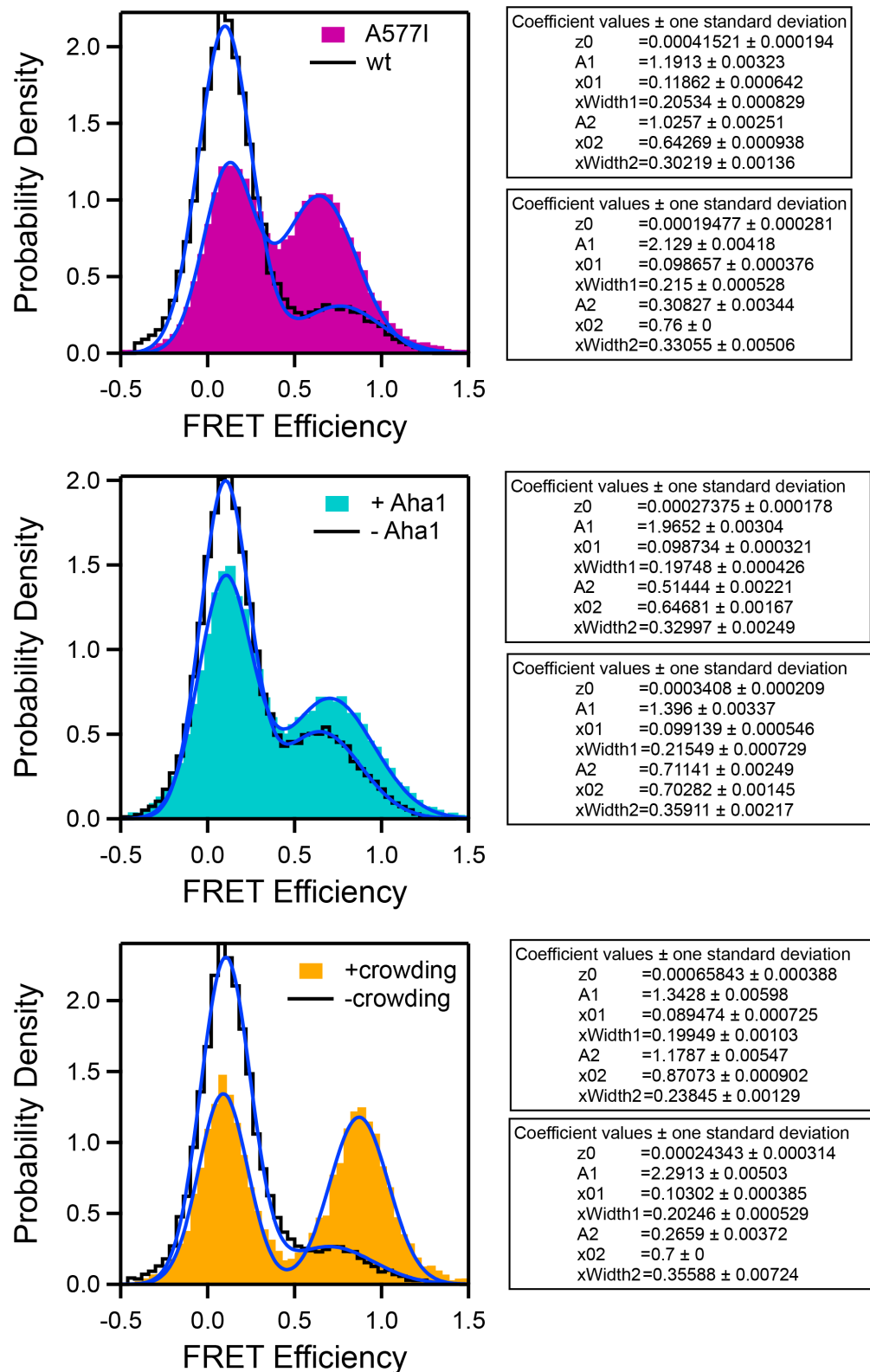


Figure 2—figure supplement 2. Fits and fit coefficients. Double-gaussian fits (blue lines) to the histograms of **Figure 2c** including fit coefficients and their standard deviations. For the smallest high-FRET populations, the peak positions x_{02} were held fixed to avoid unreasonable $x_{02} < 0.5$ (leading to standard deviation = 0). Fit function: $f(x) = z_0 + A_1 * \exp(-((x - x_{01})/xWidth1)^2) + A_2 * \exp(-((x - x_{02})/xWidth2)^2)$.

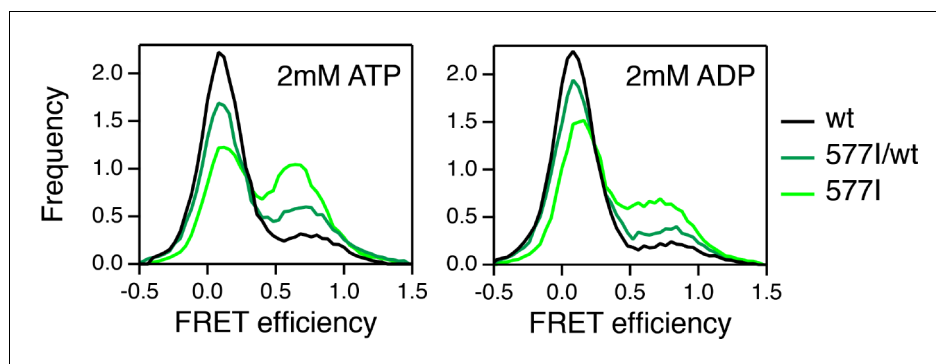


Figure 2—figure supplement 3. Single vs double A577I mutation. FRET efficiency histograms for the wild-type (wt), hetero-dimer (577I/wt) and homo-dimer (577I) show an additive effect of the A55I mutation on Hsp90's shift toward the closed conformation. Histogram integrals are normalized to unity.

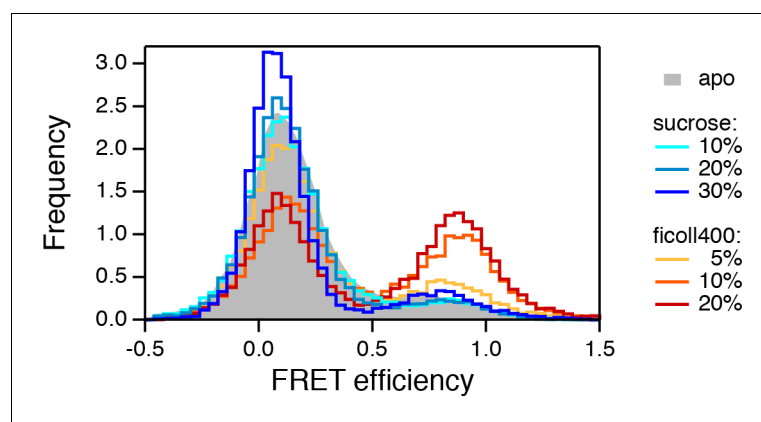


Figure 2—figure supplement 4. Macro-molecular vs small molecular crowding. FRET efficiency histograms in the absence of nucleotides (apo), and with varied weight percent sucrose or Ficoll400 show different effects on Hsp90's conformational equilibrium. Histogram integrals are normalized to unity.

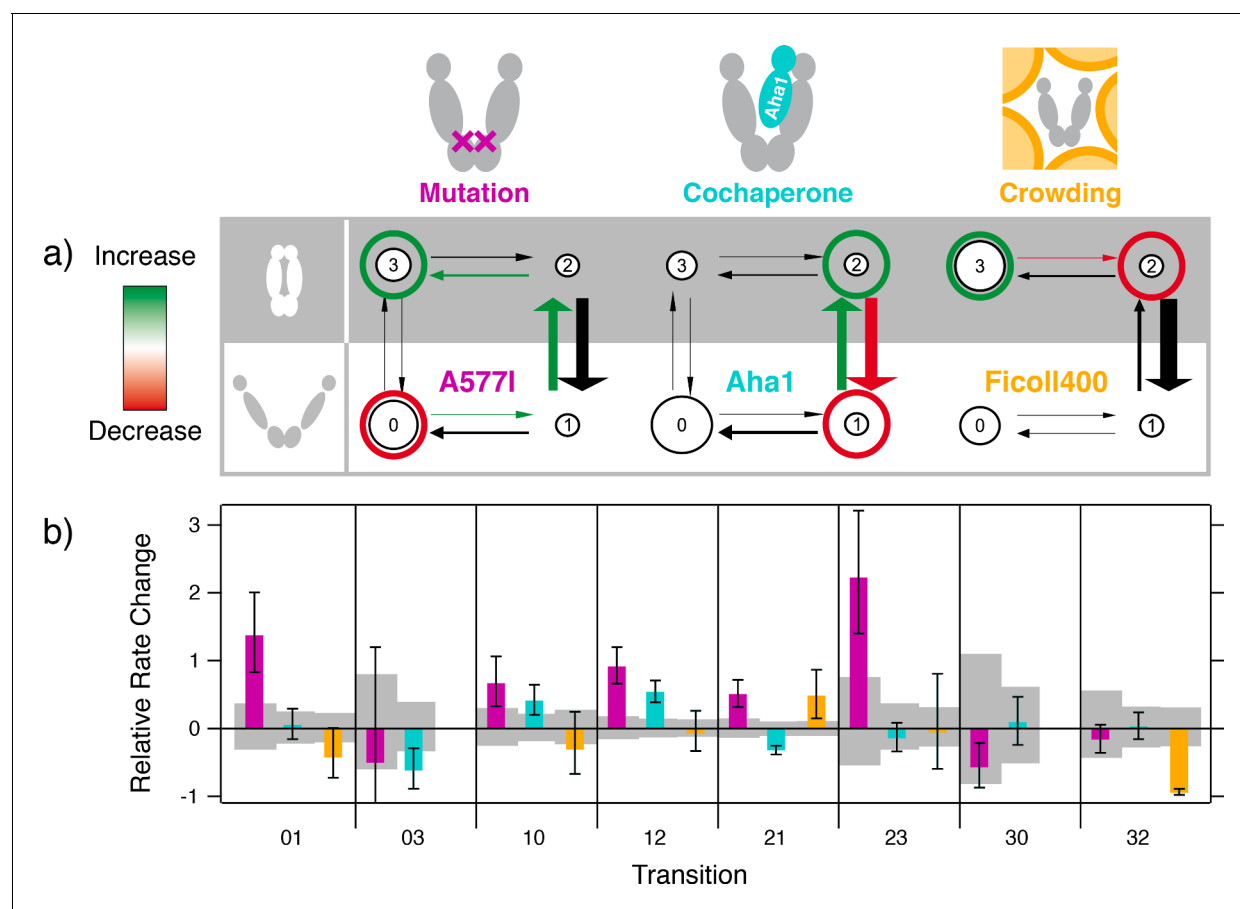


Figure 3. Different conformational kinetics cause similar thermodynamics. (a) Kinetic rate models observed for the point mutant A577I, the cochaperone Aha1, the macro-molecular crowding agent Ficoll400 - each compared to the reference data: wild-type, no Aha1, no crowding, respectively. Significant differences to the reference are highlighted in red and green. Conformational kinetics are described by four states: states 0,1 represent open conformations, and 2,3 are closed conformations. Large and small arrows and circles indicate the size of rates and populations, respectively. For crowding, only 3 links are found. (b) The relative rate change under the three conditions in (a) with respect to the reference. Gray boxes show the 95% confidence interval of the reference data. Transition names and color code as in (a). All values are listed in **Supplementary file 1C**. The molecule counts are the same as for **Figure 2**.

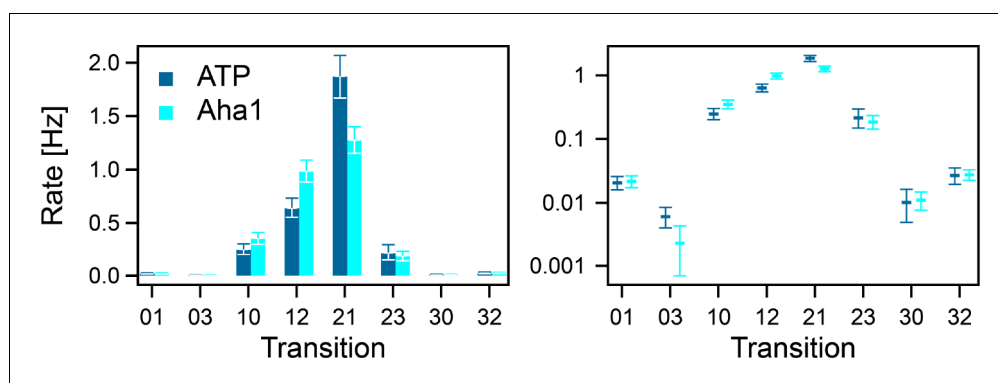


Figure 3—figure supplement 1. Rate constants and 95% confidence intervals for Hsp90 and Aha1. Results for Hsp90 in the presence of 2 mM ATP (ATP), and in the presence of 2 mM ATP + 3.5 μM Aha1 (Aha1). Left panels in linear scale, right panels in logarithmic scale.

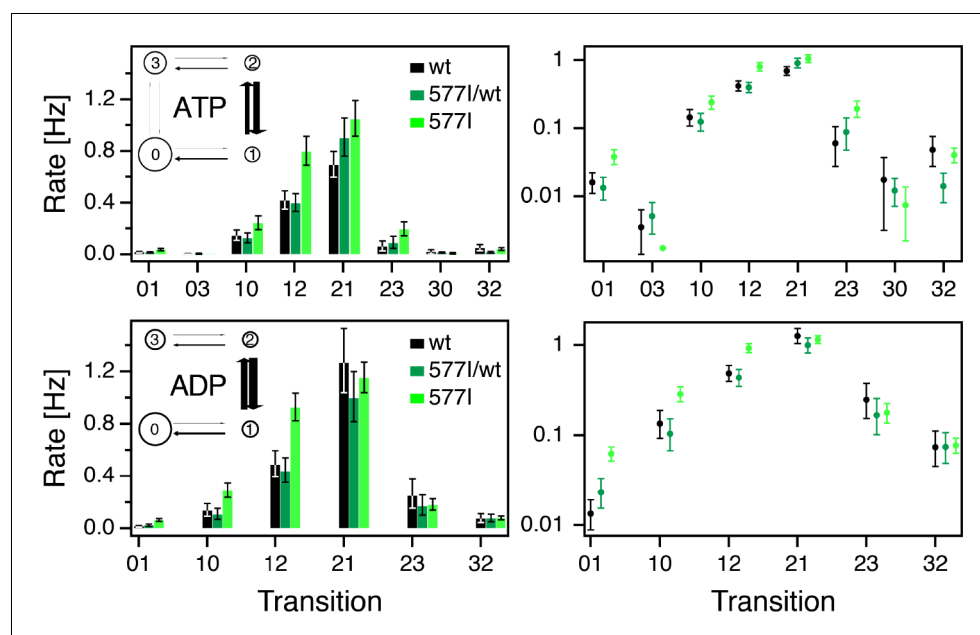


Figure 3—figure supplement 2. Rate constants and 95% confidence intervals for Hsp90 and mutations. Results for Hsp90 wild-type (wt), and the A577I hetero-dimer (577I/wt), and homo-dimer (577I), under ATP and ADP conditions as indicated. Left panels in linear scale, right panels in logarithmic scale.

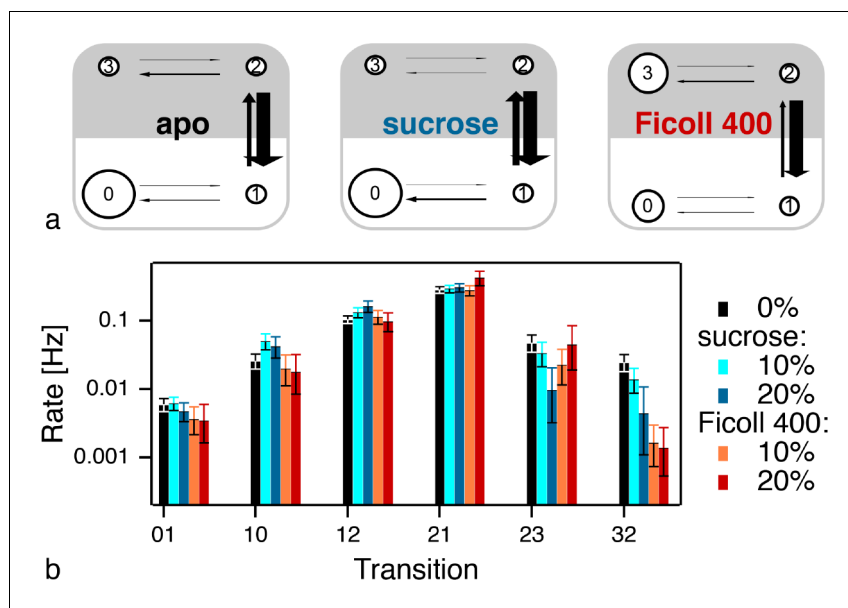


Figure 3—figure supplement 3. The effect of crowding on Hsp90's opening and closing transitions. (a) Kinetic state models for wt Hsp90 and 20% sucrose and 20% Ficoll400 (left to right): closed states, gray; open states, white; population represented by circle size; transition rate represented by arrow width. (b) Transition rates with 95% confidence intervals in logarithmic scale.

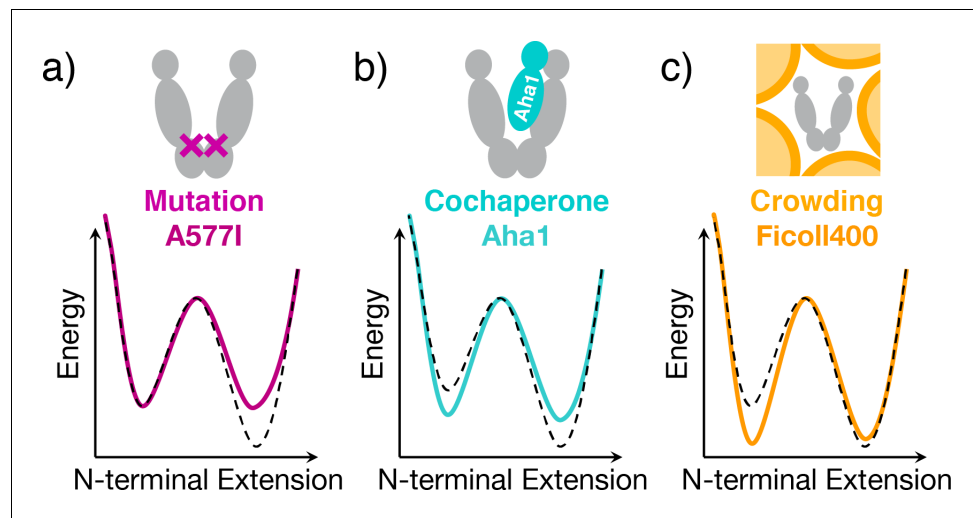


Figure 4. Three contrasting effects on Hsp90's conformational energy landscape. (a) The open conformation is destabilized by the A577I mutation. (b) Aha1 inversely affects both equilibria. (c) Macro-molecular crowding stabilizes the closed conformation. The dashed black line indicates the reference. This mechanistic information was obtained from all six rate models represented in **Figure 3**, it is not accessible from **Figure 2c** alone. To illustrate the changes on the global energy landscapes, we chose the transition state as a reference for the measured relative energies.

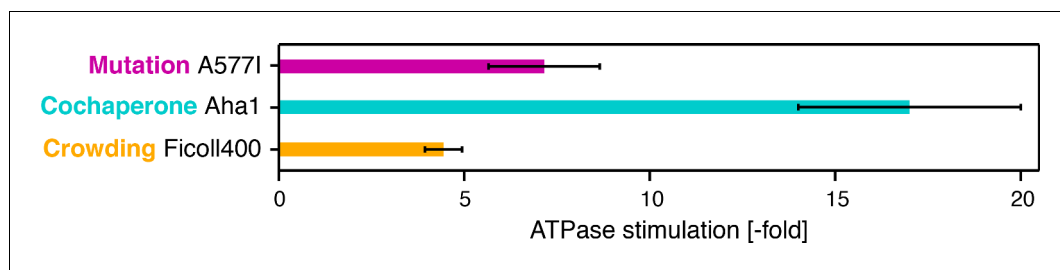


Figure 5. ATPase stimulation by local and global modulations. Namely by the point mutation A577I (*Retzlaff et al., 2009*), in the presence of 3 μ M Aha1 (*Jahn et al., 2014*) and 20wt% Ficoll400, respectively. The ATPase stimulations are normalized by the activity of the wild type, without Aha1 and without crowding, respectively.

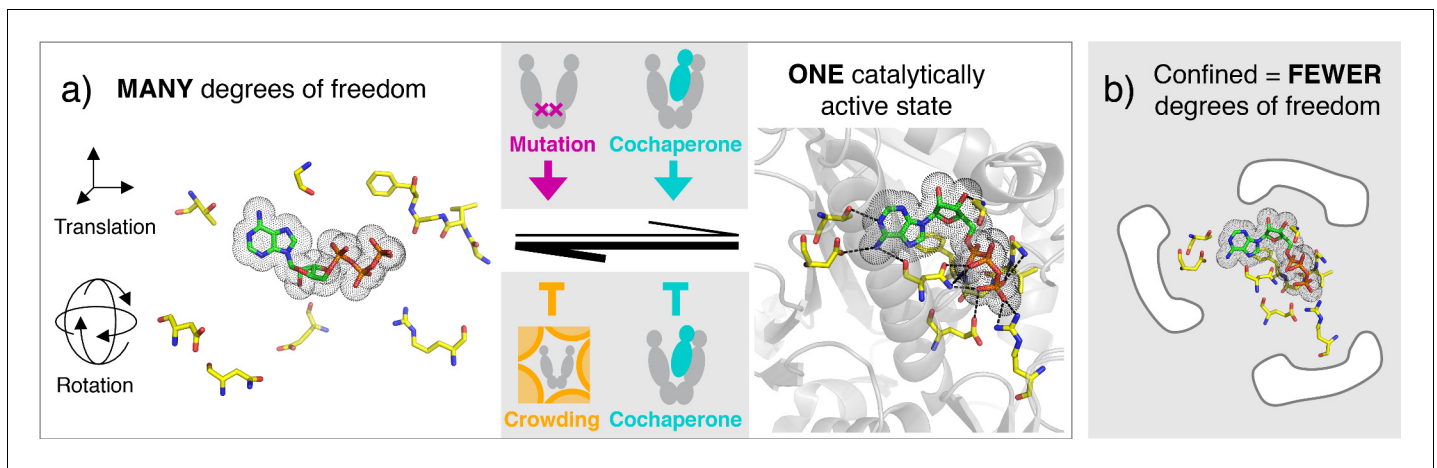


Figure 6. Stimulation of protein function by conformational confinement - a result of combinatorics. Enzymatic binding pockets of proteins are often composed of flexible elements with many degrees of freedom, (a) left. All of these have to adopt a specific 3D configuration to form the catalytically active state, (a) right. For example in Hsp90, the hydrolysis competent state includes direct contacts with residues from different domains: G100, T171, D79, N37, E33, R380, and G121-F124 (counter-clockwise from top, in the left panel). As a result, the probability to be in the catalytically active state is very small, compared to the combined probability for all other accessible conformations (left), and the catalytic activity is low. Intriguingly, specific or non-specific confinement reduces the non-productive degrees of freedom in Hsp90, leading to a relative stabilization of the hydrolysis-competent state and therefore stimulation of the catalytic activity, as illustrated in (b). Here we have shown that this can occur through allosteric effects of mutations, protein-protein interaction, or macromolecular crowding. Structures were visualized with Pymol, based on pdb entry 2cg9.